Structural basis for the neutralization and genotype specificity of hepatitis E virus

Xuhua Tang[a,1], Chunyan Yang[b,1], Ying Gu[b], Cuiling Song[b], Xiao Zhang[b], Yingbin Wang[b], Jun Zhang[b,c], Choy Leong Hew[a,c], Shaowei Li[b,c,2], Ningshao Xia[b,c,2], and J. Sivaraman[a,c,2]

[a]Department of Biological Sciences, National University of Singapore, Singapore 117543; and [b]National Institute of Diagnostics and Vaccine Development in Infectious Disease, School of Life Sciences, and [c]Xiamen-National University of Singapore Joint Laboratory in Biomedical Sciences, Xiamen University, Xiamen 361005, China

Edited by Osamu Nureki, University of Tokyo, Graduate School of Science, Bunkyo-ku, Japan, and accepted by the Editorial Board April 28, 2011 (received for review January 24, 2011)

Hepatitis E virus (HEV) causes acute hepatitis in humans, predominantly by contamination of food and water, and is characterized by jaundice and flu-like aches and pains. To date, no vaccines are commercially available to prevent the disease caused by HEV. Previously, we showed that a monoclonal antibody, 8C11, specifically recognizes a neutralizing conformational epitope on HEV genotype I. The antibody 8C11 blocks the virus-like particle from binding to and penetrating the host cell. Here, we report the complex crystal structure of 8C11 Fab with HEV E2s(I) domain at 1.9 Å resolution. The 8C11 epitopes on E2s(I) were identified at Asp^{496}-Thr^{499}, Val^{510}-Leu^{514}, and Asn^{573}-Arg^{578}. Mutations and cell-model assays identified Arg^{512} as the most crucial residue for 8C11 interaction with and neutralization of HEV. Interestingly, 8C11 specifically neutralizes HEV genotype I, but not the other genotypes. Because HEV type I and IV are the most abundant genotypes, to understand this specificity further we determined the structure of E2s(IV) at 1.79 Å resolution and an E2s(IV) complex with 8C11 model was generated. The comparison between the 8C11 complexes with type I and IV revealed the key residues that distinguish these two genotypes. Of particular interest, the residue at amino acid position 497 at the 8C11 epitope region of E2s is distinct among these two genotypes. Swapping this residue from one genotype to another inversed the 8C11 reactivity, demonstrating the essential role played by amino acid 497 in the genotype recognition. These studies may lead to the development of antibody-based drugs for the specific treatment against HEV.

Infectious viral hepatitis is a major threat to public health. Hepatitis E is one of the most important pathogenic viruses capable of infecting humans, with the highest incidence in patients aged 15 to 40 y (1). Hepatitis E infection causes severe liver inflammation, characterized by jaundice, fever, liver enlargement, and abdominal pain in humans and nonhuman primates (2). Hepatitis E virus (HEV) is prevalent in most tropical developing countries and is responsible for high rates of mortality in pregnant women by the development of fulminant liver disease (3).

The HEV genome is a positive-stranded RNA that encodes different proteins. One of these genes (ORF2) encodes a single structural protein of 660 aa, which form the capsid through its homodimeric subunits (domain E2 amino acids 394–606; domain E2s amino acids 455–602) (4, 5). These dimers are shown to protrude from the viral surface and believed to interact with host cells to initiate infection (5, 6). We recently elucidated the tertiary structure of E2s genotype I, the protruding domain of HEV, and through functional studies we have illustrated the tight homodimeric nature of E2s and identified that dimerization is essential for both HEV–host interactions and disease progression. Moreover, we mapped the neutralizing antibody recognition site of HEV on the E2s(I) domain (5).

In parallel, two crystal structures of HEV-like particles (ORF2, amino acids 112–608) were reported both at 3.5 Å for genotype III (6) and genotype IV (7). In these structural studies, three domains were defined: the shell domain (amino acids 129–319), which adopts a jelly-roll fold, and the middle (amino acids 320–455), and protrusion domains (amino acids 456–606), which both adopt a β-barrel fold. More recently, cryo-electron microscopy and image reconstructions revealed the binding of anti-HEV monoclonal antibodies to the protruding domain of the capsid protein at the lateral side of the spikes (8).

Several monoclonal antibodies against the HEV E2 domain have been raised to bind to the live HEV and affect immune capture of this virus (9). At least two of these antibodies, 8C11 and 8H3, can neutralize the infectivity of HEV. Moreover, these antibodies can act synergistically in their neutralization (9), suggesting that there are two interaction- and conformation-dependent neutralization sites on the HEV particle, which may cooperate in the adsorption and penetration of the HEV virus.

To better understand the structural basis for the neutralization mechanism, here we report the crystal structure of HEV protruding domain E2s (genotype I) in complex with the neutralization mAb 8C11 Fab, refined up to 1.9 Å. Structure-based site-directed mutagenesis was performed to identify the key residues involved in the interaction between E2s and mAb 8C11. Because 8C11 specifically recognizes the HEV genotype I and weakly binds to genotype IV, we also determined the crystal structure of E2s(IV) at 1.79 Å and generated an 8C11 complex model, and mapped the fine structural variations between the E2s(I) and E2s (IV) genotypes. Functional studies on several residues from both genotypes (I and IV) identified the key determinants that differentiate the specificity of binding. Studies on E2s-Fab complex have provided critical information on their binding specificity toward recognizing their neutralization antibody. The 8C11 epitope identified here may help in the development of antibody-based therapies for the treatment for HEV.

Results and Discussion

Overall Structure. The structure of E2s(I) in complex with the 8C11 Fab fragment was solved at 1.9 Å resolution (Table S1). In the asymmetric unit, one dimer of E2s(I) binds with two 8C11 Fab (Fig. 1) and this observation is consistent with the analytical ultra-centrifugation (AUC) results (Fig. S1). In E2s, the Fab interaction surface is located on the opposite side of the dimerization interface surface. Similar to the apo form, E2s(I) in the complex adopts the β-barrel fold and maintains a tight dimeric architecture. The 8C11-bound E2s(I) was able to be superimposed onto the unbound E2s(I) structure with an rmsd of

Author contributions: S.L. and J.S. designed research; X.T., C.Y., Y.G., C.S., X.Z., Y.W., and J.Z. performed research; X.T., C.L.H., S.L., N.X., and J.S. analyzed data; and X.T., S.L., and J.S. wrote the paper.

The authors declare no conflict of interest.

This article is a PNAS Direct Submission. O.N. is a guest editor invited by the Editorial Board.

Freely available online through the PNAS open access option.

Data deposition: The coordinates and structure factors for both E2s(I):8C11 complex and E2s(IV) have been deposited in the Protein Data Bank (accession nos. 3RKD and 3RKC).

[1]X.T. and C.Y. contributed equally to this work.

[2]To whom correspondence may be addressed. E-mail: dbsjayar@nus.edu.sg, nsxia@xmu.edu.cn, or shaowei@xmu.edu.cn.

This article contains supporting information online at www.pnas.org/lookup/suppl/doi:10.1073/pnas.1101309108/-/DCSupplemental.

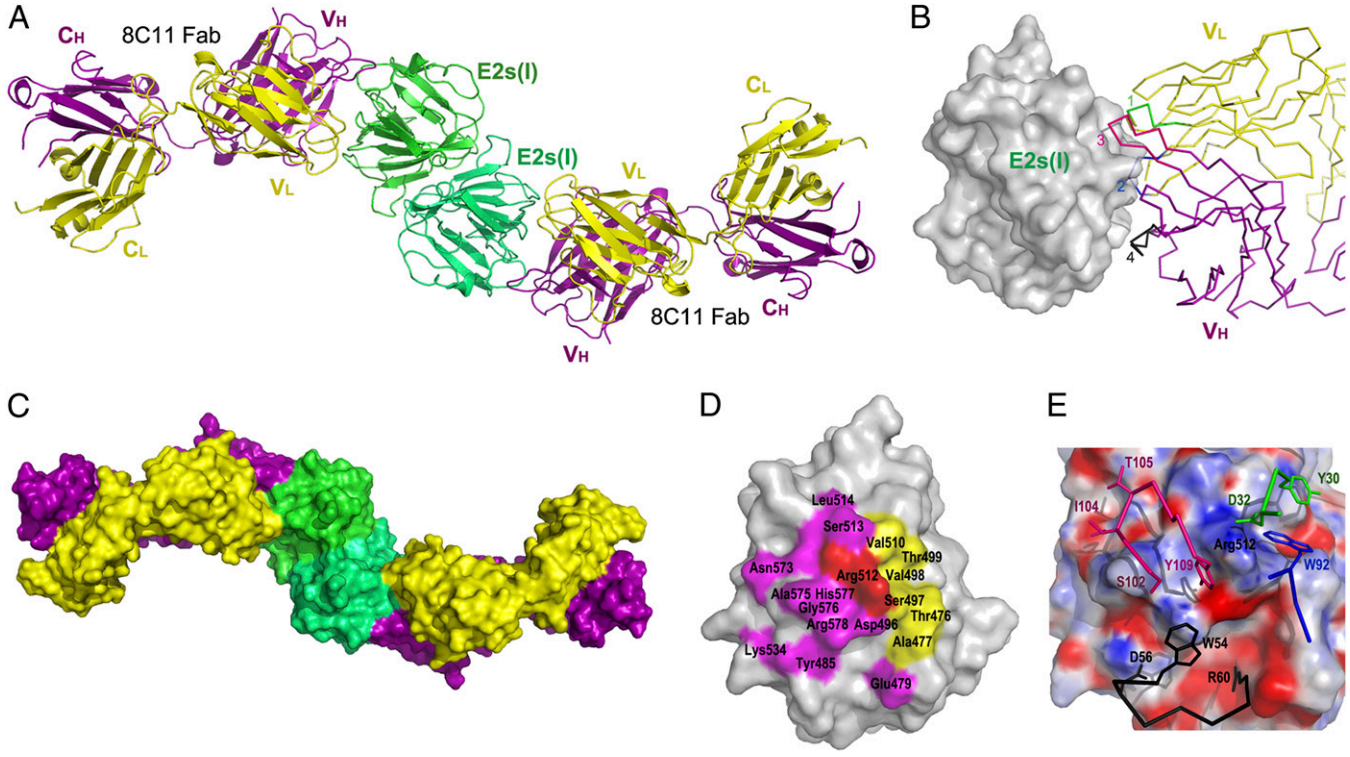

Fig. 1. Structure of E2s(I) in complex with the neutralizing antibody 8C11 Fab illustrates the neutralizing epitope. (*A*) Ribbon diagram of the E2s(I):8C11 Fab complex structure. E2s(I), 8C11 Fab heavy chain, and 8C11 Fab light chain are depicted in green (light and dark green to both monomers), purple and yellow, respectively. V_H and C_H domains of the heavy chain as well as V_L and C_L domains of the light chain are labeled. (*B*) A close-up view of the interaction of 8C11 with E2s(I) shown as surface representation. The interacting loops 1 (Tyr^{L30}-Leu^{L33}), 2 (Phe^{L91}-Asn^{L94}), 3 (Ser^{H102}-Tyr^{H109}), and 4 (Trp^{H54}-Arg^{H60}) from 8C11 were labeled and highlighted in green, blue, pink, and black, respectively. (*C*) Surface representations of E2s(I):8C11 complex structure. (*D*) Surface representations of E2s(I) highlighted the interacting epitope residues in a dark shade. The epitope residues are shown in purple and yellow corresponding to their interactions to 8C11 heavy chain and light chain, respectively. Arg^{512} is labeled in red as it interacts with both chains. (*E*) Depicts the electrostatic potential surface of the epitope on the E2s(I) (red, negative; blue, positive; and gray, neutral) with the key residues for interaction from 8C11 loops 1, 2, 3, and 4 represented as sticks. This figure and the following figures of this manuscript were prepared using the program PyMOL (27).

0.7 Å for all of the 144 Cα atoms (amino acids 459–602) by the DaliLite server (11). This finding indicates that there is no conformational change to the protruding domain E2s(I) of HEV upon binding with 8C11 Fab, and suggests that the 8C11 epitope on the E2s(I) domain has a relatively stable conformation.

In the complex, the 8C11 Fab molecule has a well-defined electron density map, except where it is disordered in the loop region in the heavy chain between Ser^{H139} and Thr^{H144}, located away from the E2s interaction surface (the superscripted "H" denotes residues within the heavy chain; a superscripted "L" will denote residues within the light chain). This region of Fab is often found disordered in other Fab structures (11). The 8C11 Fab has a canonical sandwich Ig fold (12): the heavy chain folds into V_H and C_H domains and the light chain folded with V_L and C_L domains (Fig. 1*A*).

Interactions Between E2s(I) and 8C11 Fab. The interactions between E2s(I) and 8C11 Fab buries a total of 1763 $Å^2$ of the surface area as calculated by PISA (13). Approximately 66% (or 876 $Å^2$) of the total buried surface area of E2s(I) is because of the binding of heavy chain.

A hydrophobic cluster at the binding interface consists of the side chains from Thr^{476}, Thr^{499}, and Val^{510} of E2s(I) with Trp^{L92} and Tyr^{L30} of 8C11 Fab. The hydrophobic loop region of heavy chain ^{H103}VITT^{H106} is in close contact with E2s(I) (Fig. 1 *B* and *E*). There are eight hydrogen-bonding contacts (< 3.2 Å) observed between E2s(I) and 8C11 Fab. In addition, this complex is stabilized by numerous van der Waals interactions. The specificity of 8C11 Fab to E2s(I) is dictated by three major interactions at Asp^{496}-Thr^{499}, Val^{510}-Leu^{514}, and Asn^{573}-Arg^{578} of E2s(I) (Fig. 1*D*). These observations are consistent with our previous E2s(I) mutational studies to disrupt antibody binding to this epitope (5). We showed that the mutants Glu479Ala, Tyr485Ala, and Lys534Ala significantly reduced the binding of 8C11 with E2s(I). Moreover, mutant Asp496Ala completely abrogated the interaction with 8C11. In this complex structure, hydrogen-bonding contacts were established between the side chains of all of these residues and the residues of 8C11 Fab. Notably, Arg^{512} of E2s(I) is involved in several interactions with 8C11: Arg^{512} interacted not only with 8C11 heavy chain (Thr^{H105}, Thr^{H106}, Gly^{H107}, and Tyr^{H109}) but also with the light chain (Asn^{L32} and Phe^{L91}) (Fig. 1 *D* and *E*).

Structure-Based Mutational Analysis of the Neutralizing Sites. In the E2s(I):8C11 Fab complex structure, several amino acids located on the interface were observed to interact with 8C11 Fab through their side chains, including Glu^{479}, Ser^{497}, Arg^{512}, His^{577}, Arg^{578}, and Lys^{534} of E2s(I). Structure-based functional studies were performed on the E2 constructs to determine the relevant importance of these interactions (Fig. 2). Systematically, a series of mutated E2 constructs were generated by replacing these interacting amino acids with alanine. Each construct existed mainly as a dimer in SDS/PAGE (Fig. 2*A*) and this is consistent with the AUC experiments that E2 and each mutant existed as dimers (~2.6 S) in solution (Fig. 2 *C* and *D* and Fig. S2). Only Arg512Ala abolished the interaction with 8C11 in Western blotting and in AUC experiments (Fig. 2).

To further determine the potential role of Arg^{512}, five E2 mutants were generated, replacing Arg with Glu, Leu, Lys, His, or Tyr. Similar to Arg512Ala, all of these mutants failed to interact with 8C11 mAb observed in Western blot experiments (Fig. 2*B*), although they all existed as dimers in SDS/PAGE (Fig. 2*B*) and in AUC experiments (~2.7 S) (Fig. S3). However, the

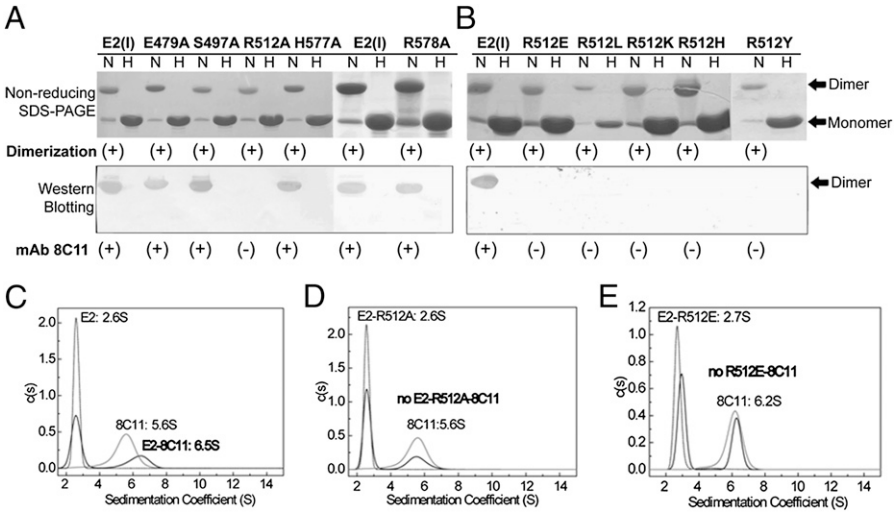

Fig. 2. Mutational studies on the E2s(I):8C11 interaction interface. (*A* and *B*) The mutants and wild-type E2 were subjected to nonreducing SDS/PAGE and Western blotting with the neutralizing mAb 8C11 to study the effects of these mutations on E2s(I):8C11 interaction. The lanes marked with H indicate heated samples in the reduced condition (i.e., these samples were heated up to 100 °C for 3 min) and the lanes marked with N indicate samples in the nonreducing condition (i.e., these samples with 0.1% SDS, no β-mercaptoethanol, and were not heated). (+) Denotes dimerization or reactivity with 8C11, (–) denotes monomer or loss of the respective property. (*C*–*E*) Sedimentation velocity (SV) was used to detect the mAb 8C11 binding of E2s(I) (*C*), and the mutants Arg512Ala (*D*) and Arg512Glu (*E*). The c(s) profile of E2, its mutants, or mAb 8C11 alone was denoted as a dashed curve. The profile of the antigen-antibody mixtures was drawn in a solid line. Molar ratio of E2 or its mutant versus mAb 8C11 was 5:1, meaning the antigen was in surplus.

AUC analysis shows that only Arg512Glu mutant abrogated the immune complex formation (Fig. 2*E* and Fig. S3). These results suggest that electrostatic interactions play a key role in mAb binding and clearly demonstrate that Arg^{512} plays a critical role in 8C11 antibody binding. The side-chain guanidine group of Arg^{512} forms hydrogen-bonding contacts (<3.0 Å) with the carbonyl oxygen (O) of Phe^{L91} and the side chain oxygen (OD1) of Asn^{L32} from the light chain of 8C11.

Cell-Binding Analysis of HEV Virus-Like Particles and Its Mutants. A recombinant mutant of HEV E2 (ORF2 amino acids 368-606), p239, which forms virus-like particles (VLPs). This particle could specifically absorb and penetrate susceptible host cells like live viruses (14). Previously, we have shown that the penetration and entry of p239 to vulnerable Huh7 cells can be blocked by either of two monoclonal antibodies: (*i*) 8C11, which recognizes a neutralizing conformational epitope; and (*ii*) 12A10, which recognizes a linear epitope located at amino acids 423–438 of E2. However, the removal of either epitope cannot completely abolish the binding capacity of p239 with Fab (15).

Based on the E2s(I):8C11 complex structure, alanine scanning mutagenesis on the interface amino acids were performed to generate constructs of p239, a truncated structural protein of HEV (VLP). All mutants maintained particulate form, comparable with the prototype p239. The cell-model assay showed that a tetra mutant, p239-Δ8C11A (Ser497Ala, Arg512Ala, His512Ala, and Arg578Ala) showed a reduced capacity to penetrate the host cell (Fig. 3*A*). However, mutating other amino acids of the 8C11 epitope on E2s had no effect (Fig. S4).

Next, we tested the penetration and entry of p239 to vulnerable cells when both 8C11 and 12A10 epitope sites were mutated. The p239 linear 12A10 epitope was substituted with tandem histidines (named as Hp239) and observed to maintain comparable entry capacity as the control p239. However, further mutation of Arg512Ala within the 8C11 binding site on Hp239 completely abrogated p239–host cell interaction (Fig. 3*B*). Therefore, the conformational 8C11 epitope and the linear 12A10 epitope are the only virus–host interaction sites; more importantly, Arg^{512}, which is located on the E2 domain, is the most crucial residue for neutralizing HEV. This finding is further supported by its strategic position of Arg^{512} and the interactions with 8C11, as revealed by the complex crystal structure.

Structure of E2s(IV) and Genotype-Specific HEV Neutralization. HEV is the only member of the genus *Hepevirus* in the family *Hepeviridae* (16). In this family, four mammalian genotypes have been identified, but with a single serotype (17). The HEV in genotypes I and II are found in humans, but those in genotypes III and IV infect both humans and swine (16).

After identifying the 8C11 epitopes on E2s(I), we sought to investigate why HEV genotype IV is not neutralized by 8C11 and to identify the key determinants, which discriminate these two most abundant genotypes. Because the E2s domain is the protruding region of HEV, which is essential for host recognition, the structural comparison between E2s types I and IV may provide the clue for their specificities toward host recognition (Fig. 4).

As a first step, the crystal structure of type IV E2s was solved at 1.79 Å resolution (Table S1). The asymmetric unit consists of an E2s(IV) dimer (Fig. 4*B*). The structural comparisons of the protruding domain of HEV from three known crystal structures of different genotypes were performed. Two high-resolution structures of the E2s domain from genotypes I and IV of this study and the 3.5 Å resolution structure of VLP from the genotype III (6) were taken for this comparison. In all three cases, a similar structure is adopted, which is consistent with there being a single serotype for four HEV genotypes. The tight dimeric architecture of E2s(I) superimpose well with the dimeric E2s(IV) and E2s(III) (Fig. 4*C*). The rmsd for pairwise comparison are 0.7 Å (between I and IV), 1.3 Å (between I and III), and 1.4 Å (between III and IV) for all Cα atoms of the E2s domain. This finding suggests that in

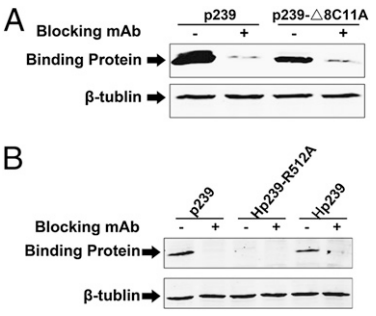

Fig. 3. Binding of VLP p239 and its mutants to Huh7 cells. (*A*) Binding of p239 and its tetra mutant p239-Δ8C11A (Ser497Ala, Arg512Ala, His512Ala, and Arg578Ala) to Huh7 cells were detected by Western blotting. With the intrinsic β-tubulin controlled in same level, p239-Δ8C11A decreased in binding capacity with respect with protype p239. (–) Denotes the absence of the blocking mAb (8G12), (+) denotes the presence of this blocking mAb. (*B*) Hp239 mutant maintains the binding capacity compared with the prototype p239. The Arg512Ala mutation on Hp239 (Hp239-Arg512Ala) construct completely abrogates cell binding.

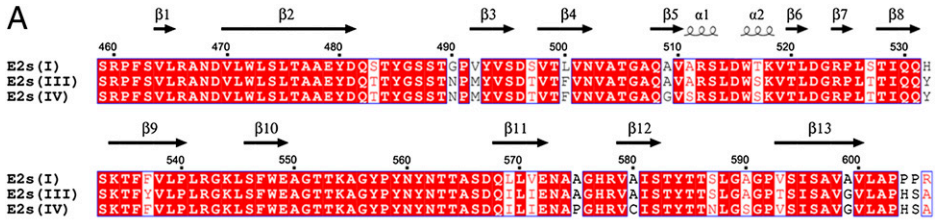

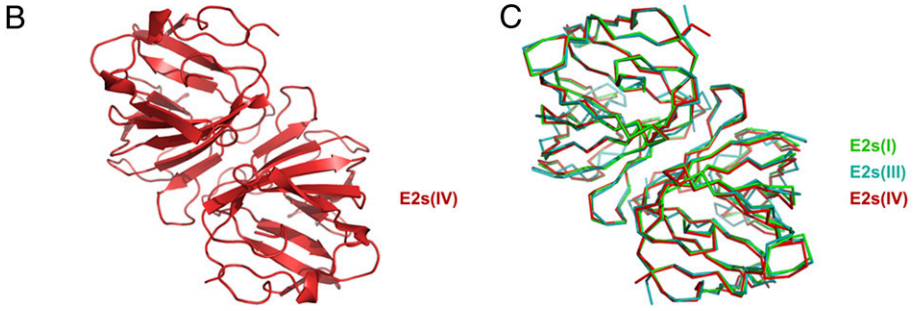

Fig. 4. Structural comparison of E2s domains across the different genotypes. (*A*) Structure-based sequence alignment between E2s genotype I, III, and IV was performed using the program COOT (23). The secondary structural elements for E2s(I) was shown and the conserved residues are highlighted in red boxes outlined in blue. This figure was created by using the program ESPript (28). (*B*) Ribbon diagram of dimeric E2s(IV) is shown in red. (*C*) Cα superposition of dimeric E2s of genotype I (green), genotype III (cyan), and genotype IV (red).

all HEV genotypes the dimerization of the protruding domain of the capsid is essential for its interactions with the host.

Type Diversity Between Genotype I and IV on the 8C11 Binding Site. To understand the specificity of mAb 8C11 toward E2s(I), the complex model of E2s:8C11 for genotype IV was generated by superimposing the E2s(IV) structure with the E2s(I) of the E2s:8C11 complex using the Dalilite server (10). The comparison between type I complex crystal structure and type IV complex model revealed the type diversity between these two genotypes in 8C11 recognition (Fig. 5). In the 8C11 epitope regions, two amino acid differences exist: genotype I contains $Ser^{497(I)}$ and $Ala^{575(I)}$, whereas genotype IV contains $Thr^{497(IV)}$ and $Pro^{575(IV)}$ [superscript "I" or "IV" denotes the residue in E2s(I) or E2s(IV), respectively] (Fig. 4*A* and 5*C*). In the E2s(I):8C11 complex, $Ser^{497(I)}$ makes a hydrogen-bonding contact with Gly^{L93} of 8C11 Fab, as well as a hydrogen-bonding contact within E2s with $Arg^{512(I)}$ (Fig. 5*B*). However, the superimposed E2s(IV):8C11 complex model reveals that the key interactions mediated through $Arg^{512(IV)}$ were completely disrupted (Fig. 5*D*): the $Arg^{512(IV)}$ side chain no longer interacted with $Thr^{497(IV)}$, and moved away from 8C11 so that it also did not interact with Asn^{L32} of 8C11. Notably, in this model the C_β group of $Thr^{497(IV)}$ is in a position to have steric clashes with Trp^{L92} of 8C11, indicating that it is not an optimal residue for this position to interact with 8C11. These observations led to the hypothesis that the residue in the amino acid 497 position is essential to differentiate between the genotypes I and IV.

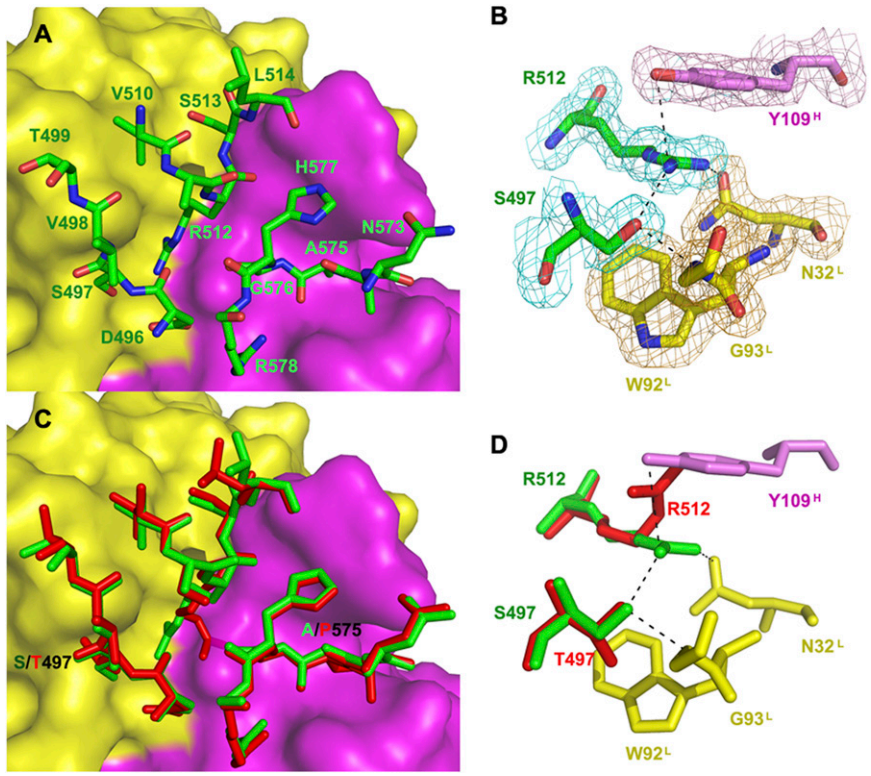

Fig. 5. Genotype specificity determinants for virus neutralization. (*A*) Three major 8C11 epitope clusters on E2s(I) are shown in ball and stick model and colored green. The 8C11 Fab was shown as surface representation. (*B*) A close-up view of the side chain of the key residue Arg^{512} interacts with Tyr^{H109} and Asn^{L32} of 8C11. Meanwhile, Arg^{512} forms a hydrogen bonding contact with Ser^{497}, which in turn interacts with Gly^{L93} of 8C11. The 2Fo-Fc map is shown and contoured at a level of 1.0σ. The hydrogen bonding contact was shown in dashed line. (*C* and *D*) Overlay of crystal structures of E2s(I) and E2s(IV) in the region of 8C11 epitope, showing the conservation and differences between these two genotypes.

To validate this hypothesis, two constructs were generated by swapping amino acid 497 on E2(I) and E2(IV): E2(I)-Ser497Thr and E2(IV)-Thr497Ser. These two mutants existed as dimers in SDS/PAGE, similar to their prototype E2(I) and E2(IV), respectively (Fig. 6*A*). In the 8C11 Western blot analysis, E2(IV)-Thr497Ser showed a significant increase in its reactivity, whereas E2(I)-Ser497Thr showed a decrease in reactivity, compared with their respective wild types (Fig. 6*A*). Moreover, the binding affinity determination (Biacore) showed that both E2(I) and E2(IV) proteins with amino acid Ser^{497} have a 2-log higher affinity than the proteins with $aaThr^{497}$ (Table 1). These results suggest that amino acid 497 plays a crucial role in 8C11 binding and HEV neutralization. Mutating Ser^{497} in E2(I) with Glu, His, Leu, Lys, or Tyr abrogated the reactivity with 8C11 observed in both Western blot and in AUC experiments (Fig. 6*B* and Fig. S5).

Based on the genotype diversity of E2, we used ELISA experiments to screen several genotype-specific mAbs that were raised previously (9). Eight antibodies that are deemed as specific genotype I antibodies were identified, and demonstrated at least a 10 times higher OD with genotype I antigens E2(I) than E2(IV) (Table 2 and Table S2). We then used the two amino acid 497 mutants [E2(I)-Ser497Thr and E2(IV)-Thr497Ser] to perform the same ELISA analysis. As shown in Table 2, four of the eight antibodies have at least a two times higher reactivity with mutant E2(IV)-Thr497Ser compared with E2-Ser497Thr (8C11, 1A5, 8E10, and 12A7). In particular, 8C11 reacted at least three times higher with E2 genotype I than genotype IV; however, the reactivity of mutant E2(IV)-Thr497Ser was higher than mutant E2(I)-Ser497Thr. It is important to note that only one residue (amino acid 497) was mutated to that of a different genotype, the reactivity of antibodies was inversed. These results demonstrate that amino acid 497 plays a crucial role in the recognition of genotype I and IV by these antibodies, including 8C11.

To visualize the binding mode of mAb 8C11 with HEV capsid, a model was generated by superimposing the E2s(I):8C11 complex onto the known models of HEV VLP (6, 7). The light chain of the Fab showed a few clashes with the middle domain of the VLP. One possibility is that the bound antibody with VLP might undergo minor conformational changes to avoid these clashes. Another possibility is the movement of the E2 domain through the loop (Q449-R460), which is connecting the protruding E2 domain and the particle shell. It is worth mentioning here that a rotation of the surface domain has been observed after the neutralizing antibody binds to dengue virus (18) and HIV-1 (19).

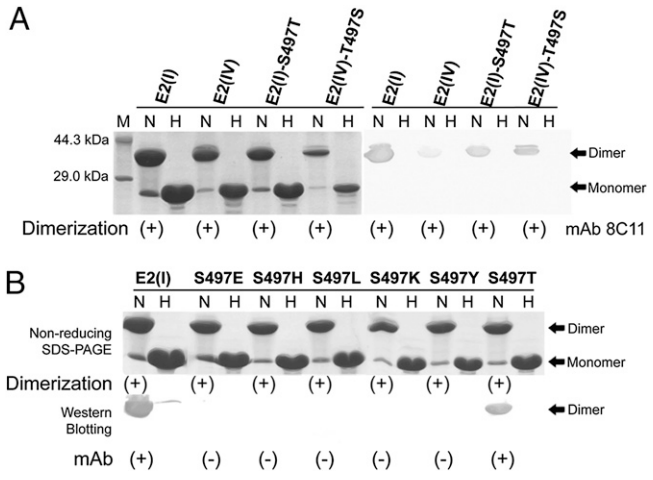

Fig. 6. The role of residue 497 in genotype-specific virus neutralization. (*A*) Wild-type E2(I) and E2(IV) as well as two amino acid 497 mutants, E2(I)-Ser497Thr and E2(IV)-Thr497Ser. (*B*) The single point mutations on Ser^{497} of E2(I) were subjected to nonreducing SDS/PAGE and Western blotting with the neutralizing mAb 8C11 to study the role of Ser^{497} involved in genotype specific definition.

Table 1. Binding kinetics of mAb 8C11 against HEV E2 type I/IV and mutants

Construct	$K_a(M^{-1}\cdot s^{-1})$	$K_d(s^{-1})$	$K_A(M^{-1})$	K_D(nM)
E2(I)	3.84×10^5	2.27×10^{-3}	1.70×10^8	5.89
E2(I)-S497T	6.53×10^3	5.00×10^{-3}	1.31×10^6	7.66×10^2
E2(IV)	3.42×10^3	2.21×10^{-3}	1.55×10^6	6.46×10^2
E2(IV)-T497S	8.46×10^4	2.37×10^{-4}	3.58×10^8	2.80

Ser497 for type I and Thr497 for type IV are strictly associated with the binding strength of mAb 8C11. The details of the Biacore experiment are described in *SI Materials and Methods*.

Conclusions

HEV is responsible for severe liver disease in humans. Infection is spreading by the fecal contamination of water supplies or food, and it is most prevalent in developing countries and countries with tropical climates. Recently, we have shown that HEV capsid protein domain E2s (protruding domain) is a homodimer and the dimerization of E2s is essential for HEV–host interactions (5). The penetration and entry of HEV to vulnerable cells can be blocked by the monoclonal antibody 8C11, which recognizes a neutralizing conformational epitope. The present study sought to elucidate the HEV:neutralizing antibody interaction to aid in the development of effective therapeutic strategies against the virus. A recombinant vaccine based on the E2s domain is in phase III clinical trials (20); however, no vaccines are commercially available for the prevention of hepatitis E. Here, we report the crystal structure of the neutralizing antibody 8C11 Fab in complex with the protruding domain of HEV capsid, E2s. The antibody 8C11 recognizes three major regions of the HEV E2s domain: Asp^{496}-Thr^{499}, Val^{510}-Leu^{514}, and Asn^{573}-Arg^{578}. Mutational analysis as well as cell-model assays demonstrated that Arg^{512} on E2s is the most crucial residue for 8C11 interaction and neutralization. The antibody 8C11 is specifically neutralizing HEV genotype I but weakly binds with other genotypes. It is worth mentioning here that type I and IV are the most abundant genotypes whereas type II is rarely observed. To understand how 8C11 discriminates different genotypes, we have determined the high-resolution structure of E2s from genotype IV at 1.79 Å resolution. Subsequently we have constructed a model of E2s(IV):8C11 and compared it with an E2s(I):8C11 complex crystal structure to identify the key determinants, which discriminate these two genotypes. We identified different residues at the 8C11 epitope region, in position amino acid 497, which plays a crucial role in the recognition of genotypes I and IV. The results presented here will lead to the designing of vaccines and specific novel inhibitors for HEV.

Materials and Methods

Cloning, Purification, Crystallization, and Structure Determination. The E2s, E2, and p239 genes of HEV genotype I were cloned (14). The equivalent E2s and E2 of HEV genotype IV were PCR-amplified from a swine HEV capsid protein gene (GenBank no. GQ166778). All mutated constructs were generated with site-directed PCR reactions. pTO-T7 expression plasmid and *E.coli* ER2566 strain were used for protein expression.

The HEV E2s(I) has been purified (5). The 8C11 Fab was obtained by papain digestion and purified with DEAE-5PW (TOSOH). The E2s(I):8C11 (ratio of 1:1.5M) was kept at 37 °C for 2 h and purified by Superdex 200 (GE Healthcare) and concentrated to ~8 mg/mL. Crystals were grown by mixing 1 μL E2s(I):8C11 with 1 μL reservoir solution (0.1M Hepes pH 7.2, 0.4 M KSCN, 0.4 M NH_4C_l, 18% PEG 3350, and 5% (wt/vol) n-Dodecyl-β-D-maltoside) using hanging-drop vapor diffusion method at 21°C. Similarly, the HEV E2s(IV) was purified, and crystals were grown from a reservoir solution consisting of 0.1 M Tris, pH 8.0 and 20% PEG 10 K. Thirty percent glycerol supplemented with reservoir condition as cryo-protectant for both crystals and data collected at 100 K. Data for crystals of E2s(I):8C11 was collected at beamline BL13B1, NSRRC, Taiwan using an ADSC Quantum-315r CCD. E2(IV) data was obtained using a CCD detector (Platinum135) mounted on a Bruker Microstar Ultra rotating anode generator. Datasets were processed by HKL2000 (21). The structures were solved by molecular replacement with PHASER (22). The models were built using COOT (23), refined by CNS (24), and analyzed by PROCHECK (25) (Table S1).

Table 2. HEV E2 type I/IV with aa497 specificity recognition in a mAb pool

	OD ratio in mAb dilution* E2(I)/E2(IV)					OD ratio in mAb dilution* E2(IV)-T497S/E2(I)-S497T				
mAb	1:100	1:1 K	1:10 K	1:100 K	Type specificity†	1:100	1:1 K	1:10 K	1:100 K	Amino acid 497 specificity†
8C11	3	9	13	12	I	1/2	2	3	3	—
1A5	6	45	81	49	I	6	10	21	6	Ser
1E8	14	6	30	57	I	1/2	1	1	2	—
3B8	38	73	4	1	I	1	1	1	1	—
8E10	4	11	29	20	I	1/2	1	3	2	—
13D8	11	5	1	1/2	I	2	2	1	1	—
6F8	8	10	2	2	I	1/100	1/17	1/4	2	Thr
12A7	4	4	6	10	I	9	10	27	56	Ser

*The 2 mg/ml mAbs were diluted at 1:100, 1:1K, 1:10K, and 1:100K as primary antibody for ELISA.
†OD ratio for E2(I)/E2(IV) and E2(IV)-T497S/E2(I)-S497T was calculated for specificity interpretation of HEV type and amino acid 497. Cutoff values were set as ≥10 or ≤1/10 for more than one of four serial dilution OD ratios.

Antibodies. The monoclonal antibodies were raised from E2(I), E2(IV), and p239 antigens using standard murine mAb preparation protocol (9).

Analytical Ultra-Centrifugation. Sedimentation velocity (SV) was used to monitor the binding of antigen and mAb in neutral solution (5). All samples were diluted to ~1.0 OD_{280nm} in 1.2-cm light path with PBS (pH 7.4). The rotor speed was set at 50,000 rpm for E2 and its mutants, 40,000 rpm for mAb 8C11, and 30,000 rpm for the immune complex. The sedimentation coefficient was obtained with c(s) method (26) using the Sedfit software kindly provided by P. Schuck (National Institutes of Health, Bethesda, MD).

Binding Assay on Cell Model. Huh7 cells (human hapatoma cell line) were incubated at 37 °C for 1 h with p239 or its mutants (20 μg) with or without preincubating with neutralizing mAb 8G12 (200 μg). The harvested cells were lysed in buffer (20 mM KOH-Hepes buffer, pH 8.0, 0.2 mM EDTA, 5% glycerol, 250 mM NaCl, 0.5% Nonidet P-40, 0.25% sodium deoxycholate, 1 mM DTT and protease inhibitors). 15B2 is the primary antibody for the Western blot, which recognizes the linear epitope HEV ORF2 aa 403–418. Alexa Fluor 680-conjugated mouse anti–β-tubulin and rabbit anti–α-tubulin (Santa Cruz Biotechnology) and Alexa Fluor 680-conjugated goat anti-mouse (Invitrogen) were then added and were examined by Odyssey (Li-COR).

ELISA Analysis. The antigen (100 ng/well) was coated in a 96-well microplate and incubated with serial dilutions of each mAb at 37 °C for 1 h. Wells were incubated with HRP-conjugated GAM for 30 min at 37 °C. Subsequently, 100 μL tetramethylbenzidine substrate was added and incubated for 10 min at 37 °C. The reaction was stopped by adding 50 μL 2 M H_2SO_4, and the OD was measured at 450 nm with a reference wavelength of 620 nm. The absorbance ratio of genotype I versus IV was calculated.

ACKNOWLEDGMENTS. We thank the Shanghai Synchrotron Radiation Facility for the help in the protein crystallization; the high-resolution datasets were collected at the National Synchrotron Radiation Research Center, Taiwan. S.L. and N.X. acknowledge funding support from the Chinese government: National Science Fund for Distinguished Young Scholars (Grant 30925030), National Natural Science Foundation (Grants 30870514, 30972826, and 30901077), Key Program in Infectious Diseases/New Drug R&D (Grants 2008ZX10004-015, 2009ZX10004-704, and 2009ZX09102-230), and Fujian Provincial Science Fund (Grants 2010Y4008, and 2009J06020); J.S. and C.L.H. acknowledge funding support from Academic Research Fund (Grant R154000438112), the National University of Singapore, Singapore.

1. Balayan MS (1993) Hepatitis E virus infection in Europe: Regional situation regarding laboratory diagnosis and epidemiology. *Clin Diagn Virol* 1:1–9.
2. Purcell RH, Emerson SU (2001) Animal models of hepatitis A and E. *ILAR J* 42:161–177.
3. Jaiswal SP, Jain AK, Naik G, Soni N, Chitnis DS (2001) Viral hepatitis during pregnancy. *Int J Gynaecol Obstet* 72:103–108.
4. Tam AW, et al. (1991) Hepatitis E virus (HEV): Molecular cloning and sequencing of the full-length viral genome. *Virology* 185:120–131.
5. Li S, et al. (2009) Dimerization of hepatitis E virus capsid protein E2s domain is essential for virus-host interaction. *PLoS Pathog* 5:e1000537.
6. Yamashita T, et al. (2009) Biological and immunological characteristics of hepatitis E virus-like particles based on the crystal structure. *Proc Natl Acad Sci USA* 106:12986–12991.
7. Guu TS, et al. (2009) Structure of the hepatitis E virus-like particle suggests mechanisms for virus assembly and receptor binding. *Proc Natl Acad Sci USA* 106: 12992–12997.
8. Xing L, et al. (2011) Spatial configuration of hepatitis E virus antigenic domain. *J Virol* 85:1117–1124.
9. Zhang J, et al. (2005) Analysis of hepatitis E virus neutralization sites using monoclonal antibodies directed against a virus capsid protein. *Vaccine* 23:2881–2892.
10. Holm L, Park J (2000) DaliLite workbench for protein structure comparison. *Bioinformatics* 16:566–567.
11. Fransson J, et al. (2010) Human framework adaptation of a mouse anti-human IL-13 antibody. *J Mol Biol* 398:214–231.
12. Al-Lazikani B, Lesk AM, Chothia C (1997) Standard conformations for the canonical structures of immunoglobulins. *J Mol Biol* 273:927–948.
13. Krissinel E, Henrick K (2007) Inference of macromolecular assemblies from crystalline state. *J Mol Biol* 372:774–797.
14. Li SW, et al. (2005) Mutational analysis of essential interactions involved in the assembly of hepatitis E virus capsid. *J Biol Chem* 280:3400–3406.
15. He S, et al. (2008) Putative receptor-binding sites of hepatitis E virus. *J Gen Virol* 89: 245–249.
16. Purcell RH, Emerson SU (2008) Hepatitis E: An emerging awareness of an old disease. *J Hepatol* 48:494–503.
17. Worm HC, van der Poel WH, Brandstätter G (2002) Hepatitis E: An overview. *Microbes Infect* 4:657–666.
18. Lok SM, et al. (2008) Binding of a neutralizing antibody to dengue virus alters the arrangement of surface glycoproteins. *Nat Struct Mol Biol* 15:312–317.
19. Liu J, Bartesaghi A, Borgnia MJ, Sapiro G, Subramaniam S (2008) Molecular architecture of native HIV-1 gp120 trimers. *Nature* 455:109–113.
20. Zhu FC, et al. (2010) Efficacy and safety of a recombinant hepatitis E vaccine in healthy adults: A large-scale, randomised, double-blind placebo-controlled, phase 3 trial. *Lancet* 376:895–902.
21. Otwinowski Z, Minor W (1997) Processing of X-ray diffraction data collected in oscillation mode. *Methods Enzymol* 276:307–326.
22. Storoni LC, McCoy AJ, Read RJ (2004) Likelihood-enhanced fast rotation functions. *Acta Crystallogr D Biol Crystallogr* 60:432–438.
23. Emsley P, Cowtan K (2004) Coot: Model-building tools for molecular graphics. *Acta Crystallogr D Biol Crystallogr* 60:2126–2132.
24. Brünger AT, et al. (1998) Crystallography & NMR system: A new software suite for macromolecular structure determination. *Acta Crystallogr D Biol Crystallogr* 54: 905–921.
25. Laskowski RA, Macarthur MW, Moss DS, Thornton JM (1993) PROCHECK: A program to check the stereochemical quality of protein structures. *J Appl Cryst* 26:283–291.
26. Schuck P (2000) Size-distribution analysis of macromolecules by sedimentation velocity ultracentrifugation and lamm equation modeling. *Biophys J* 78:1606–1619.
27. Delano W (2002) *The PyMOL Molecular Graphics System* (Delano Scientific, San Carlos, CA).
28. Gouet P, Courcelle E, Stuart DI, Métoz F (1999) ESPript: Analysis of multiple sequence alignments in PostScript. *Bioinformatics* 15:305–308.